

## Preequilibrium escape widths of giant resonances

M. O. Roos,<sup>1,2</sup> H. Dias,<sup>2</sup> O. Rodriguez,<sup>2,\*</sup> N. Teruya,<sup>3</sup> and M. S. Hussein<sup>2</sup>

<sup>1</sup>*Departamento de Física, Universidade Federal de Mato Grosso, 78069-000, Cuiabá, MT, Brazil*

<sup>2</sup>*Instituto de Física da Universidade de São Paulo, 05389-970, São Paulo, SP, Brazil*

<sup>3</sup>*Departamento de Física, Universidade Federal da Paraíba, 58051-970, João Pessoa, Pb, Brazil*

(Received 3 January 2001; revised 20 May 2002; published 28 August 2002)

In this work we present a calculation of the  $2p$ - $2h$  preequilibrium escape width of giant resonances for the nuclei  $^{40}\text{Ca}$ ,  $^{90}\text{Zr}$ , and  $^{208}\text{Pb}$ . The problem studied here involves an excited nucleus in the  $1p$ - $1h$  configuration, evolving to the  $2p$ - $2h$  configuration with the  $1p$  in the continuum. The theoretical approach used for our calculations is based on the statistical multistep compound theory of Feshbach, Kerman, and Koonin (FKK) and on the particle-hole state densities given by Obložinský. Our calculations show that although different state densities supply a similar result for the damping width, the escape width is strongly dependent on the nuclei, on the binding energy of the emitted nucleon, and the excitation energy of the giant resonance.

DOI: 10.1103/PhysRevC.66.024611

PACS number(s): 21.60.-n, 24.30.Cz, 24.60.Dr

### I. INTRODUCTION

The study of the decay properties of giant multipole resonances (GRs) on collective and statistical doorways [1] demonstrated the statistical nature of the decay process. The GRs are located at high excitation energies and they mainly decay by particle emission. Treated as isolated resonances, the GRs are characterized by a total average width composed of two pieces: the escape width, which represents the coupling of the GRs to the continuum, and the damping width, which measures the degree of fragmentation of the strength due to coupling to complex intrinsic nuclear configurations (e.g.,  $2p$ - $2h$ ). The first stage of the reaction (the giant resonance population) is a coherent process in which  $1p$ - $1h$  configurations act in phase; the next stages are more complicated and require a statistical treatment. It is important to mention that quite recently statistical aspects of nuclear coupling to continuum was developed [2]. In a previous publication [3] the damping width of the GRs using the FKK [4,5] and the Obložinský approach [6,7] was calculated and similar results for both approaches were found. In this paper we extend the analysis to the escape width.

This paper is organized as follows. In Secs. II and III we present the basic ideas for calculating the decay widths. The analytical comparison between FKK and Obložinský approaches for damping width is given in Sec. IV. The analytical and numerical calculations for escape width are given in Sec. V. Finally, in Sec. VI, the results of calculations and conclusions are presented.

### II. THEORETICAL FOUNDATIONS

The statistical multistep compound nuclei theory (MSC) of Feshbach, Kerman, and Koonin [4,5] gives for the total width ( $\Gamma_{nJ}$ ) of a given giant resonance with angular momentum

$J$ , excitation energy  $E$ , and in a configuration neighboring the  $n$ th stage of the decay chain

$$\langle \Gamma_{nJ} \rangle = \langle \Gamma_{nJ}^{\downarrow} \rangle + \langle \Gamma_{nJ}^{\uparrow} \rangle, \quad (1)$$

where  $\langle \Gamma_{nJ}^{\downarrow} \rangle$  is the width of damping and  $\langle \Gamma_{nJ}^{\uparrow} \rangle$  is the escape width, corresponding to the emission of a nucleon with a simultaneous creation of a pair particle-hole, with no change in the number of excitons or with an annihilation of a particle-hole pair respectively (see details in [5]).

Within considerations of model [5], it is assumed that the interaction between excitons is a force of the type

$$V(\mathbf{r}_1, \mathbf{r}_2) = V_0 \left( \frac{4}{3} \pi r_0^3 \right) \delta(\mathbf{r}_1 - \mathbf{r}_2), \quad (2)$$

where  $V_0$  is an overall strength and  $r_0 = 1, 25$  fm is the nuclear radius constant.

For the calculation of the widths one still assumes factorization in the energy and the angular momentum dependencies of the density of states. For the escape all the involved widths in the process of emission of nucleons assume the form

$$\langle \Gamma_{nJ}^{j_s \nu}(U) \rho_{s\nu}(U) \rangle = X_{nJ}^{j_s \nu}(U) Y_n^{\nu}(U). \quad (3)$$

The  $Y$  functions contain all the dependence on excitation energy which originates from the final density of levels, while the  $X$  functions contain the structure of angular momentum included in  $\delta$ -force and the spin distribution function of the single-particle levels. In the case of the escape width, the  $X$  function also leads to a dependence on excitation energy due to the fact that the width depends on the state of the residual nuclei characterized by energy  $U$  and spin  $s$ .

### III. STRUCTURE OF ENERGY AND ANGULAR MOMENTUM

For the process corresponding to the emission of a nucleon with a simultaneous creation of a particle-hole pair, the  $X$  and  $Y$  functions are schematically shown in the Fig. 1. In these diagrams, the double strings denote the nucleon leading to the compound system, arrows going up (descend)

\*Also at Instituto Superior de Ciências y Tecnología Nucleares, Av. Salvador Allende y Luaces, Apartado Postal 6163, La Habana, Cuba.

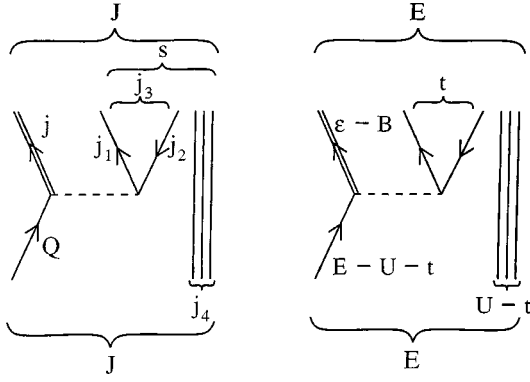


FIG. 1. Diagrammatic representation of the angular momentum coupling ( $X$  function) and of the energy representation ( $Y$  function) for the  $\Delta n = +1$  escape process.

represent particles (holes), the hatched strings represent the residual interaction, and the three vertical strings represent excitons that do not participate in the interaction.

The expression for the  $Y$  function for escape, according to FKK theory, is given by

$$Y_n^{n+1}(U) = g(gE)\xi^N, \quad (4)$$

where  $\xi = U/E$ . The expression for damping, also according to FKK theory, is given in [4] and is schematically represented by the same diagram for ( $Y_n^{n+1}(U)$ ), except that the double arrow must be replaced by a simple arrow, representing an emitted nucleon.

Another approach for these functions was proposed by Obložinský [6,7]. According to Obložinský, using the same notation as above, the  $Y$  functions for escape are given by

$$Y_n^{n+1}(U) = \frac{1}{2} \frac{g^3}{\omega(p, h, E)} \frac{\omega(p, h-1, U^N)}{N(N-1)}. \quad (5)$$

In these expressions, the particle-hole density  $\omega(p, h, E)$  is given by

$$\omega(p, h, E) = \frac{g^N}{p!h!(N-1)!} \sum_{i=0}^p \sum_{k=0}^h (-1)^{i+k} \binom{p}{i} \binom{h}{k} \Theta(E - \alpha_{ph} - iB - kF) (E - A_{ph} - iB - kF)^{N-1}, \quad (6)$$

where  $B$  is the binding energy and  $F$  is the Fermi energy,

$$\alpha_{ph} = \frac{1}{2} \left( \frac{p^2 + p}{g} + \frac{h^2 - h}{g} \right), \quad (7)$$

$$A_{ph} = \frac{1}{2} \left( \frac{p^2 + p}{g} + \frac{h^2 - 3h}{g} \right), \quad (8)$$

and, for the remaining densities, using a compact notation,

$$\omega(p, h, U^{N+v}) = \begin{cases} \frac{g^{p+h}}{p!h!(N-1)!} \sum_{i=0}^p \sum_{k=0}^h (-1)^{i+k} \binom{p}{i} \binom{h}{k} \\ \times \Theta(U - iB - kF) (U - iB - kF)^{N+v} & \text{for } U > 0 \\ 0 & \text{for } U \leq 0. \end{cases} \quad (9)$$

The expression for the  $X$  function for escape, including the spin dependence of interacting excitons, is given by

$$X_{nJ}^{js(n+1)}(U) = 2\pi \frac{(2j+1)(2s+1)}{R_N(J)} \sum_{Qj_3j_4} (2Q+1)F \\ \times (j_3)(2j_3+1)R_1(Q)R_{N-1}(j_4) \\ \times \begin{pmatrix} j & Q & j_3 \\ \frac{1}{2} & -\frac{1}{2} & 0 \end{pmatrix}^2 \begin{Bmatrix} j & j_3 & Q \\ j_4 & J & s \end{Bmatrix}^2 \\ \times I^2(j_1, j_2, j_3, J) \Delta(QJj_4), \quad (10)$$

where the angular momentum density of a pair is

$$F(j_3) = \sum_{j_1j_2} (2j_1+1)R_1(j_1)(2j_2+1)R_1(j_2) \\ \times \begin{pmatrix} j_1 & j_2 & j_3 \\ \frac{1}{2} & -\frac{1}{2} & 0 \end{pmatrix}^2, \quad (11)$$

the triangle delta function,  $\Delta(j_a j_b j_c)$ , ensures angular momentum conservation, and the  $R_N(J)$  functions are given by equation

$$R_N(J) = \frac{(2J+1)}{\pi^{1/2} N^{3/2} \sigma^3} e^{-(J+1/2)^2/N\sigma^2}, \quad (12)$$

where the single-particle spin cutoff parameter ( $\sigma$ ) is given by [4]

$$\sigma = \left[ \frac{\sqrt{12} A^{5/3}}{45\pi g} \right]^{1/2} \quad (13)$$

and  $g$  is the single-particle level density.

The radial overlap integrals of the single-particle wave functions are

$$I(j_1, j_2, Q, j) = \left( \frac{4}{3} \pi r_o^3 \right) V_o \frac{1}{4\pi} \\ \times \int_0^\infty R_{j_1}(r) R_{j_2}(r) R_Q(r) R_j(r) \frac{dr}{r^2}, \quad (14)$$

where the functions  $R_j(r)$  are the radial parts of harmonic oscillator wave functions.

#### IV. COMPARISON BETWEEN FKK AND OBLOŽINSKÝ APPROACHES FOR THE CALCULATION OF THE DAMPING WIDTHS

A numerical comparison of the damping widths given by the FKK and the Obložinský approaches is presented by Ceneviva *et al.* [3], where it is shown that the two methods give similar results. The difference in these calculations comes basically from energy and level density factor dependencies, explicitly in the  $Y^\downarrow$  function, since the factor that contains the geometric dependence (angular momentum), the  $X^\downarrow$  functions, are the same for the formalisms studied.

Our intention in this section is to summarize the result of [3] by showing analytically that in the region of GRs (between 10 and 20 MeV) these two approaches supply the same results approximately in calculating the damping width, namely,

$$\frac{Y_{\text{Obložinský}}^\downarrow}{Y_{\text{FKK}}^\downarrow} \approx 1, \quad (15)$$

where  $Y_{\text{FKK}}^\downarrow = g(gE)^2/2(N+1)$ .

It is sufficient to remember that in all the cases studied so far  $F > E$  and thus all the terms containing  $(E - F)$  will go to zero due to the fact that the Heaviside function appearing in Eq. (9) has a negative argument (consequently  $k$  always will be null there). Further, in general  $B < E < 2B$ , therefore the maximum number of particles in Eq. (9) will be one ( $p_{\text{max}} = 1$ ).

Thus, substituting  $h = 1$  and  $p = 1$  in the expressions for  $\omega(p, h, U^{n+\nu})$  necessary for calculating the function  $Y^\downarrow$  of Obložinský, we have

$$Y_{\text{Obložinský}}^\downarrow = \frac{1}{12} g^3 E^2 \frac{3B - E}{B}. \quad (16)$$

Therefore, the ratio between the  $Y$  functions of Obložinský and FKK is

$$\frac{Y_{\text{Obložinský}}^\downarrow}{Y_{\text{FKK}}^\downarrow} = \frac{1}{2} \frac{(3B - E)}{B}. \quad (17)$$

In general  $B \leq E \leq 2B$  (depending on the nuclei and the type of particle) and the ratio shown above will have values between 1.0 and 0.5, respectively.

#### V. ESCAPE WIDTH

The escape width is defined by

$$\langle \Gamma_{nJ}^\uparrow \rangle = \sum_{\nu=n-1}^{n+1} \sum_{js} \int_0^{E-B} \langle \Gamma_{nJ}^{js\nu}(U) \rho_{s\nu}(U) \rangle dU. \quad (18)$$

The simplest way to perform the calculation of this expression is to first sum over all spins of the residual nuclei,  $s$ , and then evaluate the energy integral. Summing over  $s$ , and applying the completeness of  $6-j$  coefficients, the  $X$  function becomes independent of the residual nuclei and can be expressed by

$$X_{nJ}^{\uparrow n+1} = 2\pi \sum_{jQj_3j_4} (2j+1)F(j_3)(2j_3+1) \frac{R_1(Q)R_{N-1}(j_4)}{R_N(J)} \\ \times \begin{pmatrix} j & Q & j_3 \\ \frac{1}{2} & -\frac{1}{2} & 0 \end{pmatrix}^2 I^2(j_1, j_2, j_3, J) \Delta(QJj_4). \quad (19)$$

On the other hand, using appropriate the  $Y$  function in Eq. (18) and integrating over the energy of the residual nuclei, we can write

$$\langle \Gamma_{nJ}^\uparrow(E) \rangle = Y_n^{\uparrow n+1}(E) X_{nJ}^{\uparrow n+1}, \quad (20)$$

for which, in the FKK approach, we have

$$Y_n^{\uparrow n+1}(E) = Y_{\text{FKK}}^\uparrow = \int_0^{E-B} g(gE) \frac{U^N}{E^N} dU = g^2 \frac{(E-B)^{N+1}}{E^{N-1}(N+1)}. \quad (21)$$

On the other hand, the Obložinský approach, using the same considerations, gives

$$Y_n^{\uparrow n+1}(E) = Y_{\text{Obložinský}}^\uparrow \\ = \int_0^{E-B} \frac{1}{2} \frac{g^3}{\omega(p, h, E)} \frac{\omega(p, h-1, U^N)}{N(N-1)} dU \\ = \frac{1}{2} \frac{g^2}{BN(N-1)} \left\{ \frac{(E-B)^{N+1}}{(N+1)} - \frac{(E-2B)^{N+1}}{(N+1)} \right\}. \quad (22)$$

Taking  $N = 2$  in expressions (21) and (22), it follows that

$$\frac{Y_{\text{Obložinský}}^\uparrow}{Y_{\text{FKK}}^\uparrow} = \frac{E}{4B} \left[ 1 - \left( \frac{E-2B}{E-B} \right)^3 \right], \quad (23)$$

and a simple direct comparison between the FKK and the Obložinský formalisms for the total escape widths can be made in analogy with the damping process. The results are presented in Table I for some values of  $E$ . A comparison of numerical calculations will be presented in the next section.

TABLE I. Comparison between the  $Y$  function in FKK ( $Y_{\text{FKK}}^\uparrow$ ) and Obložinský ( $Y_{\text{Oblo}}^\uparrow$ ) approaches for preequilibrium escape.

$\frac{E}{B}$	2	1.5	1.4	1.3	1.2	1.1
$\frac{Y_{\text{Oblo}}^\uparrow}{Y_{\text{FKK}}^\uparrow}$	0.5	0.75	~1.4	~4.5	~20	~200

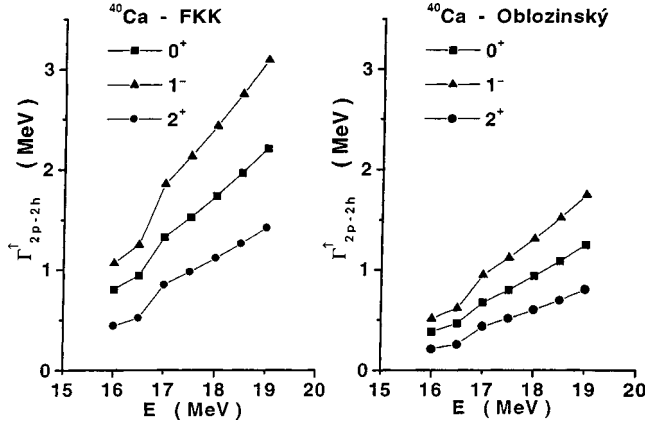


FIG. 2. Escape widths ( $1p-1h \rightarrow 2p-2h$ ) for the  $E0$ ,  $E1$ , and  $E2$  GR's in  $^{40}\text{Ca}$ .

## VI. RESULTS AND CONCLUSIONS

We present, in Figs. 2, 3, and 4, the results of the calculations of the escape width for the region of the giant resonances in the nuclei  $^{40}\text{Ca}$ ,  $^{90}\text{Zr}$ , and  $^{208}\text{Pb}$ , respectively.

The single-particle level density is defined by  $g = (6/\pi^2)a$ , where  $a$  is a parameter related to the excitation energy and nuclear temperature [4,9]. We adopted  $a = A/10$ , in the oscillator harmonic approach [9], for  $^{40}\text{Ca}$  and  $^{90}\text{Zr}$ , obtaining  $g = 2.43$  and  $5.47 \text{ MeV}^{-1}$ , respectively. These densities are in reasonable agreement with estimates of Dilg *et al.* [10]. For  $^{208}\text{Pb}$ , we used  $a = 10.02$  [10], with a corresponding value of  $g = 6.09 \text{ MeV}^{-1}$ .

The single-particle space configuration must be defined so as to simulate, in some way, the continuum part of the spectrum, whose states the emitted nucleon will be able to occupy. The chosen states of single-particle and single-hole from each nucleus had been those generated from a Woods-Saxon spherical potential in a base of harmonic oscillator using the DENCON code [11], with the parameters shown in Table II.

The maximum energy in the single-particle spectrum ( $\epsilon_{\max}$ ) depends on the excitation energy ( $E$ ), the binding energy of the nucleon ( $B$ ), and the minimum energy necessary for the creation of a particle-hole pair ( $\xi_{ph}$ ), or

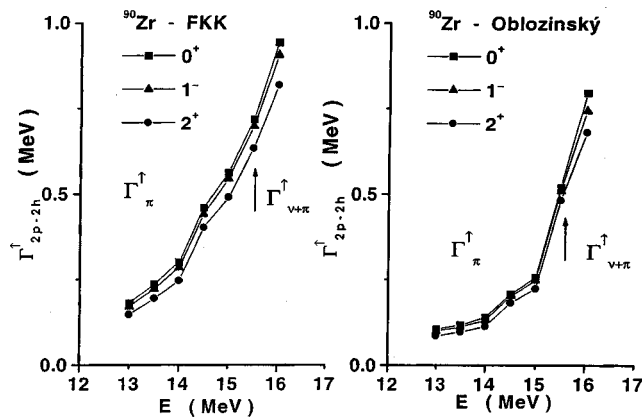


FIG. 3. Escape widths ( $1p-1h \rightarrow 2p-2h$ ) for the  $E0$ ,  $E1$ , and  $E2$  GR's in  $^{90}\text{Zr}$ .

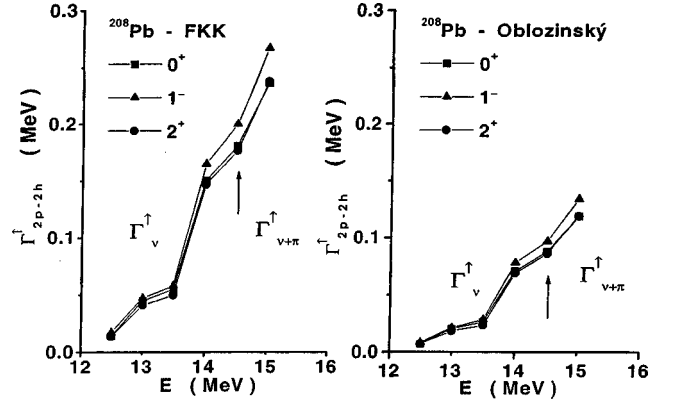


FIG. 4. Escape widths ( $1p-1h \rightarrow 2p-2h$ ) for the  $E0$ ,  $E1$ , and  $E2$  GR's in  $^{208}\text{Pb}$ .

$$\epsilon_{\max} = E - B - \frac{\xi_{ph}}{2}, \quad (24)$$

where  $\xi_{ph}$  is calculated using the theoretical values of the binding energies:

$$\xi_{ph} = B(A, X) - B(A+1, X+1), \quad (25)$$

where  $X = Z$  or  $N$  depending on the calculated value of  $\xi_{ph}$  for protons or neutrons. Note that if  $E < B + \xi_{ph}/2$ , no nucleon emission will occur, depending on the nuclei, the binding energy of the nucleon emitted, and the excitation energy of the resonance. The theoretical values of  $\xi_{ph}$  calculated with the adjusted single-particle spectra coincide with the experimental data. Our calculations indicate that, in the case of  $^{40}\text{Ca}$ , proton emission dominates the escape; for  $^{90}\text{Zr}$ , both protons and neutrons are emitted with neutron escape occurring from  $\sim 15.5$  MeV, and in  $^{208}\text{Pb}$  neutron emission dominates the process with a small contribution of proton emission from  $\sim 14$  MeV. Then preequilibrium protons are also emitted in  $^{40}\text{Ca}$  besides the usual semidirect protons.

The damping (escape) widths are calculated by adding the contributions of the protons and of the neutrons:

$$\Gamma_{2p-2h}^{\downarrow(\uparrow)} = X_{2p-2h}^{\downarrow(\uparrow)\pi} Y_{2p-2h}^{\downarrow(\uparrow)\pi} + X_{2p-2h}^{\downarrow(\uparrow)\nu} Y_{2p-2h}^{\downarrow(\uparrow)\nu}. \quad (26)$$

The proton (neutron) contributions are defined in agreement with the initial pair particle-hole is formed by protons (neutrons) and their respective holes. As demonstrated in Sec. II, the ratio  $Y_{\text{Oblozinsky}}^{\downarrow}/Y_{\text{FKK}}^{\downarrow}$  is limited between 1.0 and 0.5 in agreement with the energy of the excitation,  $B \leq E \leq 2B$ , respectively. In the damping process, all of the  $X$  functions used in the two approaches are independent of the excitation energy and are exactly the same for protons or for neutrons, respectively. This happens due to the fact that the chosen space configuration is constant and identical. Although some ratios among the  $Y$  functions are small, the contributions for the width are amplified or reduced through the  $X$  functions and there will be a dominant term in Eq. (26). In this way,

TABLE II. Set of parameter values for the Woods-Saxon potential used in the calculations. The symbols  $\pi$  ( $\nu$ ) refer to the protons (neutrons),  $\lambda$  denotes the strength of the spin-orbit potential, and  $\kappa$  is used in the parametrization of the depth of the central potential as defined in [11].

Nucleus		$V_0$ (MeV)	$r_0$ (fm)	$r_{so}$ (fm)	$\lambda$	$\kappa$	$a_0$ (fm)	$a_{so}$ (fm)
$^{40}_{20}\text{Ca}_{20}$	$\nu$	55.650	1.195	1.240	22.80	0.63	0.63	0.63
	$\pi$	55.590	1.200	1.240	19.90	0.63	0.63	0.63
$^{90}_{40}\text{Zr}_{50}$	$\nu$	53.625	1.240	1.240	29.09	0.63	0.625	0.63
	$\pi$	53.638	1.240	1.240	17.80	0.63	0.624	0.63
$^{208}_{82}\text{Pb}_{126}$	$\nu$	49.600	1.347	1.280	31.50	0.86	0.70	0.70
	$\pi$	49.600	1.275	0.932	17.80	0.86	0.70	0.70

through the compensation in the products  $XY$  appearing in  $\Gamma_{2p-2h}^\dagger$ , the damping width calculations in these two approaches give similar results. In the case of the escape, however, the space configuration changes due to the coupling of a particle to the continuum linked to the excitation energy through Eq. (24). On the other hand, the ratio  $Y_{\text{Obložinský}}^\dagger/Y_{\text{FKK}}^\dagger$  has the behavior shown in Table I. The incorporation of these last two effects produces the results obtained in Sec. V.

As regards the behavior of the escape width as a function of the excitation energy, one can notice that  $\Gamma_{2p-2h}^\dagger(E)$  increases with energy, while points seemingly appear singular where there are “breaks” in the monotonicity of the curves. The explanation for such behavior is in the single-particle space configuration in the continuum and in the  $Y$  functions, interpreted here as the total density of the states.

For  $^{40}\text{Ca}$ , the space configuration in the continuum is  $(2p_{3/2}, 2p_{1/2})^\pi$  up to  $\sim 16.5$  MeV and the inclusion of the state  $(1f_{5/2})^\pi$  starting from  $\sim 17$  MeV does not change the behavior of the GR widths significantly, although it corresponds to a contribution of  $\sim 18\%$ ,  $22\%$ , and  $30\%$  for the resonances  $0^+$ ,  $1^-$ , and  $2^+$ , respectively. Note that  $\epsilon_{\text{max}}^\nu < 0$ , so that the system does not have sufficient energy to eject neutrons.

For  $^{90}\text{Zr}$ , the possible single particle states in the continuum are  $(3s_{1/2}, 2d_{3/2})^\pi$  up to  $\sim 14$  MeV,  $(3s_{1/2}, 2d_{3/2}, 1h_{11/2})^\pi$  from  $\sim 14$  to  $16$  MeV, and  $(2f_{7/2})^\nu$  starting from  $\sim 15.5$  MeV and  $(2f_{7/2}, 3p_{1/2})^\nu$  starting from  $\sim 16$  MeV. The behavior of  $\Gamma_{2p-2h}^\dagger(E)$  is explained not only in the geometry of the problem, but also in the competition between the functions  $Y_{\text{FKK}}^\dagger$  and  $Y_{\text{Obložinský}}^\dagger$ . The  $Y$  functions, in the FKK approach, are increasing functions for protons and for neutrons. In the approach of Obložinský, these functions are increasing functions for protons and decreasing for neutrons. What happens is that up to  $\sim 15$  MeV only protons can be emitted and a proportionality between the  $\Gamma_{\text{FKK}}^\dagger$  and  $\Gamma_{\text{Obložinský}}^\dagger$  widths can be established ( $\Gamma_{\text{FKK}}^\dagger \sim 2 \times \Gamma_{\text{Obložinský}}^\dagger$ ). This is directly related to the fact that  $Y_{\text{FKK}}^\dagger \sim 2 \times Y_{\text{Obložinský}}^\dagger$  in this energy region. When we increased the space of neutrons starting from  $\sim 15.5$  MeV, the contribution of neutrons for the escape width becomes very significant ( $\sim 50\%$  of the total escape width). This happens because at  $\sim 15.5$  MeV,  $Y_{\text{Obložinský}}^\dagger \sim 5 \times Y_{\text{FKK}}^\dagger$ . Then, the competition between the decaying open channels explains the behavior of  $\Gamma_{2p-2h}^\dagger(E)$ .

For  $^{208}\text{Pb}$ , in spite of  $\epsilon_{\text{max}}^\pi \approx 4$ ,  $9$  MeV with the  $(2g_{9/2}, 1i_{11/2})^\pi$  proton space being valid only from  $\sim 14$  to  $15$  MeV, there is no significant contribution for the escape widths inside the energy interval considered. For neutrons we have  $(2h_{11/2}, 4p_{3/2})^\nu$  single-particle states at  $\sim 12.5$  MeV and with the inclusion of the states  $(4p_{1/2}, 3f_{7/2})^\nu$  at the energy of  $\sim 13.5$  MeV, we have a behavior similar to that of the  $^{40}\text{Ca}$  at  $\sim 17$  MeV. The space configuration increases then starting from  $\sim 14$  MeV with the incorporation of the levels  $(3f_{5/2}, 1k_{19/2})^\nu$  and at  $\sim 15$  MeV with the level  $(1j_{13/2})^\nu$ , without significant change in the behavior of  $\Gamma_{2p-2h}^\dagger(E)$ .

Another effect that appears in the graphs, especially in  $^{40}\text{Ca}$ , is that the escape widths of resonances with  $J=1$  are significantly larger than the widths with  $J=0$ , while it is expected that the total escape width decreases with the increase of the angular momentum. We have emphasized that our study is referring to GR decay from  $1p-1h$  to  $2p-2h$ , in the process that includes the escape of a proton or a neutron and we only considered resonances with natural parity. In this context, resonances with the same parity exhibit this type of behavior, besides for  $^{40}\text{Ca}$ . In the usual shell model, the parity of the shells alternates basically in a systematic way. In the single-particle spectra at low energy (approximately near to the  $sd$  shell), the coupling of angular momenta with different parity favors the escape of the resonant states with negative parity, and for this reason the escape width with  $J=1^-$  it is larger than the one with  $J=0^+$  for the  $1p-1h$  to  $2p-2h$  decay process. For  $^{90}\text{Zr}$  and  $^{208}\text{Pb}$ , the shells near the Fermi energy already contain states of single particle with blended parities, in such a way that this effect becomes less apparent.

In this work, we analytically demonstrated that using the formalism of Obložinský for the particle-hole level densities [6,7], the damping widths gives results similar to those obtained using the theory developed by Feshbach, Kerman, and Koonin [4]. We also demonstrate analytically and numerically that the same conclusion cannot be applied to the process of escape and a more rigorous study must be performed in which the proper approach must be chosen. In Table III we present some calculated values of these widths in comparison with the total and damping widths for some resonances. In light nuclei, the contribution of the escape width to the population of  $2p-2h$  levels in the residual nucleus is more apparent than in heavy nuclei [8,12,13], because the statisti-

TABLE III. Escape width calculations on the centroid of GRs in comparison with an estimate of total width [1] and the damping width [3].

Nucleus	GR	$E_x$ (MeV)	$\Gamma$ (MeV)	$\Gamma^\downarrow$ (MeV) [3]	$\frac{\Gamma_{2p-2n}^\uparrow \text{ (MeV)}}{\text{FKK Oblo}}$		$\frac{\Gamma^\uparrow}{\Gamma}(\%)$ [1]
					FKK	Oblo	
$^{40}\text{Ca}$	E2	$\sim 17.5$	$\sim 3.0$	1.2	0.98	0.51	$\geq 50$
$^{90}\text{Zr}$	E0	$\sim 16.1$	$3.1 \pm 0.4$	2.4	0.98	0.80	10–20
$^{208}\text{Pb}$	E0	$\sim 13.5$	$3.0 \pm 0.5$	3.8	0.06	0.03	10–15

cal process is the principal decay mechanism, contributing with  $\sim 90\%$ . Finally, we have shown that preequilibrium decay of GRs in  $^{40}\text{Ca}$  is predominantly through the proton channel.

#### ACKNOWLEDGMENTS

This work was partially supported by the PICDT/CAPES Program of UFMT and by CNPq-CLAF.

- 
- [1] H. Dias, M. Hussein, and S. K. Adhikari, Phys. Rev. Lett. **57**, 1998 (1986).
- [2] S. Drożdż, J. Okolowicz, M. Płoszajczak, and I. Rotter, Phys. Rev. C **62**, 024313 (2000).
- [3] C. A. P. Ceneviva, N. Teruya, H. Dias, and M. Hussein, Phys. Rev. C **57**, 3220 (1998).
- [4] H. Feshbach, A. K. Kerman, and S. Koonin, Ann. Phys. (N.Y.) **125**, 429 (1980).
- [5] R. Bonetti, M. B. Chadwick, P. E. Hodgson, B. V. Carlson, and M. H. Hussein, Phys. Rep. **202**, 171 (1991).
- [6] P. Obložinský, Nucl. Phys. **A453**, 127 (1986).
- [7] P. Obložinský and M. B. Chadwick, Phys. Rev. C **42**, 1652 (1990).
- [8] C. A. P. Ceneviva, N. Teruya, H. Dias, and M. Hussein, Phys. Rev. C **55**, 1246 (1997).
- [9] A. Bohr and B. R. Mottelson, *Nuclear Structure* (Benjamin, New York, 1969), Vol. 1.
- [10] W. Dilg, W. Shantl, H. Vonach, and M. Uhl, Nucl. Phys. **A217**, 269 (1973).
- [11] F. Garcia, O. Rodriguez, E. Garrote, and V. Rubchenya, Comput. Phys. Commun. **86**, 129 (1995).
- [12] M. Kohl, P. von Neumann-Cosel, A. Richter, G. Schrieder, and S. Strauch, Phys. Rev. C **57**, 3167 (1998).
- [13] H. Diesener *et al.*, Phys. Rev. Lett. **72**, 1994 (1994).